Atlantis Highlights in Engineering, volume 4

13th International Renewable Energy Storage Conference (IRES 2019)

Numerical Assessement of Energy Storage Performances of Magnetite and Quartzite for CSP Storage Applications

Yousra FILALI BABA*
3ER Team, Department of Energy,
Ecole Nationale Supérieure d'Arts et Métiers
Moulay Ismail University
Meknès, Morocco
filalibabayousra@gmail.com

Ahmed AL MERS
3ER Team, Department of Energy,
Ecole Nationale Supérieure d'Arts et Métiers
Moulay Ismail University
Meknès, Morocco
almers_a@hotmail.com

Hamid AJDAD
3ER Team, Department of Energy,
Ecole Nationale Supérieure d'Arts et Métiers
Moulay Ismail University
Meknès, Morocco
ajdad.cmi@gmail.com

Yaroslav GROSU
CIC Energigune, Albert Einstein 48,
Miñano, Álava 01510, Spain
ygrosu@cicenergigune.com

Abdessamad FAIK
CIC Energigune, Albert Einstein 48,
Miñano, Álava 01510, Spain
afaik@cicenergigune.com

*Corresponding author

***Abstract*—this paper pinpoints the thermal energy storage performances of two TESM, quartzite as classic thermal energy storage material commonly used in CSP and magnetite as emerged thermal energy storage filler material. The TES performances included charge, discharge and cycle efficiencies (utilization rate). In the first place, the developed numerical code for thermocline energy storage is presented and validated. Subsequently, and for both filler materials, the thermocline behavior and TES performances during charging and discharging process are examined. These performances are investigated for two potential scenarios: the first one considers the same storage tank size and the same discharge period. While, the second one, concerned sized storage tank for each combination HTF/TESM. Different heat transfer fluids are utilized involving natural oils, synthetic oils and molten salt. The obtained results showed that no significant difference of the zone thickness between the two materials. Moreover, we noted that quartzite presents slightly higher charge discharge and storage efficiencies. However, magnetite, for the same storage tank size and the same discharge time, magnetite is able to restore a great amount of energy. Furthermore, magnetite requires less storage tank volume. More important, we deduced that the TES performances are not impacted only by the TESM properties but they are also driven by the HTF nature and that molten salts are largely more efficient**.

Keywords—thermocline energy storage; TESM; HTF; magnetite; quartzite; thermocline behavior; charge efficiency; discharge efficiency; storage efficiency.

I. INTRODUCTION

Two tanks storage and thermocline packed-bed single tank concept fall into the category of sensible heat storage systems, nevertheless thermocline technology seems to draw attention to other systems because of its cost effectiveness in comparison with two tanks system [1] [2] [3]. Feedbacks have demonstrated that storing energy via this technology can be considered both as a promising outcome and a real challenge for cost effective thermal energy storage, intended to capture and store energy when available and discharge this energy on demand. [4]. It has also shown that reaching an efficient energy storage and sustainable management of thermal process is conditioned by multiple criteria involving:

- High energy density in the TESM;
- Good heat transfer between HTF and TESM;
- Mechanical and chemical stability of the TESM;
- Compatibility between the HTF, the TESM and the storage tank;
- Low thermal losses, etc. [5]

So far, several TESMs have been chosen and evaluated as potential candidates for thermal storage using thermocline technology, among other, we mention: quartzite [6] [7] [8] [9], concrete [10] [11] [12],granite [13] [14], basalt[15], alumina[16] [17] [18], cofalite[19] [20], graphite [21] [22], and gabbro [15]. Some of these materials fulfill several criteria cited above as the quartzite and gabbro. Others represent advantages but also disadvantages like concrete [23]. But in most of cases, these materials are derived from natural rocks that can give them the advantage of being more stable and low cost due to their abandonment in the nature. However, face to this diversity of choice offered to interested industrialists and researchers, it seems that the TESM which has been distinguished among others TESM is the quartzite. This filler material has been widely used in the most CSP installations emerged to date. This material was distinguished not only for its thermophysical properties compared to other TESM derived from natural rocks, but also for its mechanical stability and its compatibility with the most of heat transfer fluids commonly used in the CSP applications.

On the other hand, several studies are conducted to identify other TESMs that can replace quartzite or that represent better characteristics [15] [18]. The research for these new TESM candidates is motivated not only by technical constraints but also by logistical considerations. Because, usually we opt for

the TESM available near the installation sites. The research carried out since then has made it possible to identify other TESM materials that represent thermophysical properties that can compete with quartzite, among which we find magnetite that has recently gained growing interest for the thermocline energy storage applications. Presented as promising material filler, it has been demonstrated that this natural ore offers excellent properties, reversible latent heat transition and controlled thermal conductivity [24]. More important, magnetite ore remains an ecofriendly, available and cost effective materials. But in that sense, no rigorous comparison with quartzite, considered as reference TESM, has been made until now to demonstrate the real potential of magnetite. Given the importance that this comparison may represent for the concerned community, we propose in this work the comparison between the performances of the two TESMs which can be considered as the best way to confirm the advantages and disadvantages not only of magnetite but also those of quartzite.

The present work is devoted to the comparison in terms of thermocline storage performances based on numerical simulation. For this purpose, a numerical code based on dual phase model is developed and validated. It is used to simulate the behavior of charging and discharging for quartzite and magnetite, and then to evaluate their performances by calculating discharge and storage efficiencies.

II. THERMOCLINE STORAGE PERFORMANCES NUMERICAL COMPARISON BETWEEN MAGNETITE AND QUARTZITE

A. Mathematical model

The storage model concerns heat exchange between the different components of the storage tank, Thereby, it allows the prediction of the thermocline behavior, and hence the evaluation of the performances for both quartzite and magnetite coupled with different heat transfer fluids commonly used in this field. Dual phase model is adopted [8] [9]. It is based on heat and mass balance and considers that the packed-bed contained in the storage tank as continuous mediums, formed by two distinct systems: the HTF designed by "f"', the TESM "s" and the metallic wall designed by "p". The storage tank is considered as a vertical cylinder that contains a packed bed constituted of quartzite or magnetite with a HTF flowing through the void fraction "$\mathcal{E}$", In this model, HTF and TESM exchange heat with each other through the volumetric heat transfer coefficient "hv" [25]. whereas the metallic wall exchanges heat from its inside with the HTF and TESM through the areal heat transfer coefficient "hp" [26] and exchanges heat with the surrounding medium from its outside via the heat transfer coefficient "hext".

B. Model assumptions

The aforementioned model is established under the following assumptions:

- Unidirectional heat transfer;
- Transitional regime for temperature;
- Homogenous porous matrix, with spherical particles;
- Radiant heat transfer is neglected.

C. Governing equations

The governing equations for the fluid designed by "f", the solid designed by "s" and the wall designed by "p" are as follow:

- Energy balance for HTF:

$$\varepsilon\rho_f Cp_f\left(\frac{\partial T_f}{\partial t}+U\frac{\partial T_f}{\partial x}\right)=\varepsilon\lambda_f\frac{\partial^2 T_f}{\partial x^2}+hv(T_s-T_f)+hp\frac{A_{fp}}{V_f}(T_p-T_f) \quad (1)$$

- Energy balance for TESM:

$$(1-\varepsilon)\rho_S Cp_S\left(\frac{\partial T_S}{\partial t}\right)=(1-\varepsilon)\lambda_S\frac{\partial^2 T_S}{\partial x^2}+hv(T_f-T_S)+hp\frac{A_{sp}}{V_S}(T_p-T_S) \quad (2)$$

- Energy balance for the metallic wall:

$$\rho_p Cp_p\left(\frac{\partial T_p}{\partial t}\right)=\lambda_p\frac{\partial^2 T_p}{\partial x^2}+hp\frac{A_{fp}}{V_p}(Tp-T_f)+hp\frac{A_{sp}}{V_p}(T_p-T_S)+hext\frac{A_{pext}}{V_p}(T_p-T_{ext}) \quad (3)$$

Asp, Afp, Apext, represent respectively the surface contact ratio between the three components of storage tank: TESM-metallic wall, HTF-wall and wall-surrounding medium, while U refers to the fluid velocity calculated based on the mass flow rate $\dot{m}$: $U=\frac{4\dot{m}}{\pi D^2 \varepsilon \rho_f}$

For the boundary conditions, during the charging process, the hot fluid enters the tank from the top, this corresponds to an adiabatic condition for the solid and the metallic wall, and the hot HTF leaves the tank from the bottom which correspond to an adiabatic condition for the fluid the solid and the wall. During the discharging process; the same adiabatic boundary conditions are maintained for the metallic wall and the TESM. Except for the HTF, the conditions are inversed, where the temperature is imposed at the entrance (x=0) and the adiabatic condition are considered at the exit (x=H).

D. Numerical resolution

The numerical resolution of the different equations of the model was performed using the finite difference method (FDM) with a second order central differencing scheme for the second order derivative terms, a central differencing scheme for the first order derivative terms and an implicit scheme for the time discretization. It was solved by the Tridiagonal matrix algorithm (TDMA) and an iterative procedure. For each cycle (charge, discharge), the stopping of charging or discharging phases is conditioned by the Tcut-off or breakout temperature defined by:

$$T_{cut-off}(charge)=T_L+\delta\,(T_H-T_L) \quad (4)$$

$$T_{cut-off}(discharge)=T_H-\delta\,(T_H-T_L) \quad (5)$$

The coefficient δ is usually defined according to the temperature required by the process using the discharged energy. Then the condition for stopping the charging process

is: $T_f^{output} \leq T_{cut-off}$ and for the discharging process: $T_f^{output} \geq T_{cut-off}$.

E. Model validation

An experimental reference considered as one of the most remarkable case in the literature is presented here: CNRS-PROMES demonstrator. It consists of thermocline packed-bed single tank filled of rapeseed oil as HTF and quartzite as TESM. More details or specifications in reference [8][26]. The confrontation between experimental and numerical results is presented in Fig. 1. The temperature distribution from the numerical model appears to be in a satisfactory agreement with experimental data, the corresponding average difference between experimental and numerical results does not exceed 1°C.

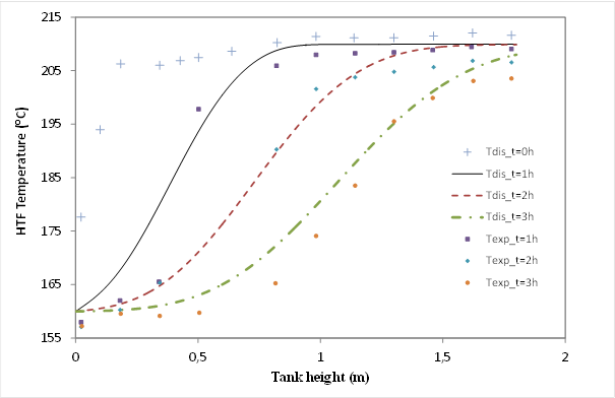

Fig. 1. Comparison between the dual phase model results and experimental data from CNRS-PROMES [8] [26]

III. THERMOCLINE STORAGE PERFORMANCES SPECIFICATIONS

The storage tank considered here corresponds to the SIROCCO project [27] the framework project of this study. The objective is to develop a solar boilers technology based on Fresnel solar concentrating system [27] coupled with thermocline storage system.

The gross capacity power of the storage system is 100 kWth with autonomy of 5 hours. Table I summarizes the specifications of the single tank thermocline system, and the Table II presents the thermal and thermophysical properties of the HTF/TESM candidates, whereas the

Table III recapitulates the used parameters of each combination. Based on this approach, it becomes possible to evaluate quartzite and magnetite.

For each combination TESM/HTF comparison, the parameters, the most relevant for characterizing the thermocline storage performances are considered:

The energy absorbed by the heat transfer fluid during the discharge period, it is expressed as:

$$E_{f,dis,f} = \int_{t=t_{char}}^{t=t_{dis}} m_{f,dis} C_{pf} (T_f(x_0,t) - T_f(H,t)) dt \quad (6)$$

The discharge efficiency defined as the ratio of the energy delivered to the heat transfer fluid and the ideal discharged energy corresponding to the ideal thermocline profile [10].

$$\eta_{dis\_rate} = \frac{E_{f,dis,f}}{E_{ideal}} \quad (7)$$

The ideal discharged energy is calculated based on the expression:

$$E_{ideal} = V\left(\epsilon\, \rho_f\, C_{pf} + (1-\epsilon)\, \rho_s\, C_{ps}\right)(T_H - T_L) \quad (8)$$

The cycle efficiency defined as the ratio of the energy absorbed by the heat fluid during discharge and the energy delivered by the heat transfer fluid during charge. It is expressed as:

$$\eta_{cycle} = \frac{E_{f,dis}}{E_{f,char}} \quad (9)$$

TABLE I. CHARACTERISTICS OF THE STORAGE TANK

Thermal Energy Storage Technology	**Single Tank Thermocline system: Sirocco project**
Discharge hours (h)	5
Gross capacity (kWth)	100
Temperature range (°C)	175-210
Heat Transfer fluid	Colza Oil / Delco Term Oil / Syltherm Oil / Hitec XL/ Hitec HTS
Thermal Energy Storage material	Quartzite / Magnetite
H/D	2
Particle diameter (m)	0,01
Porosity	0,4

TABLE II. CHARACTERISTIC OF SOME HEAT TRANSFER FLUIDS STUDIED: THE AVERAGE VALUE OF EACH PARAMETER IS DETERMINED FOR THE RANGE OF TEMPERATURE BETWEEN 170°C AND 210°C

HTF/TESM Characteristics	**Colza Oil**	**Delco Term E15**	**Hitec XL**	**Quartzite**	**Magnetite**
Density (kg/m3)	787,7	671	2081	2500	4962
Thermal heat capacity (J/kgK)	2492	2726	1488	830	850
Thermal conductivity (W/mK)	0,143	0,118	0,519	3,155	3,1

TABLE III. OPTIMAL CHARACTERISTICS OF THE STORAGE TANK OBTAINED FOR SOME DIFFERENT COMBINATIONS HTF/TESM ACCORDING TO SIROCCO PROJECT SPECIFICATIONS

	Combinations	**Solid volume (m^3)**	**Fluid volume (m^3)**	**Tank volume (m^3)**	**Tank Diameter (m)**	**Mass flow rate (Kg/s)**
(g)	Quartzite + Hitec XL	17,146	11,430	28,5	2,63	2,64
(h)	Magnetite + Hitec XL	11,297	7,531	18,8	2,28	2,64

IV. RESULTS

A. Temperature profile and thermocline height for charging and discharging process

This section examines, numerically, the behavior of magnetite and quartzite during charging and discharging processes. The analysis of the temperature profile of the HTF during the charging or discharging period is very impressive because the shape of the HTF temperature profile makes it possible to deduce the height of the thermocline zone reflecting the storage performance of the pair TESM/HTF.

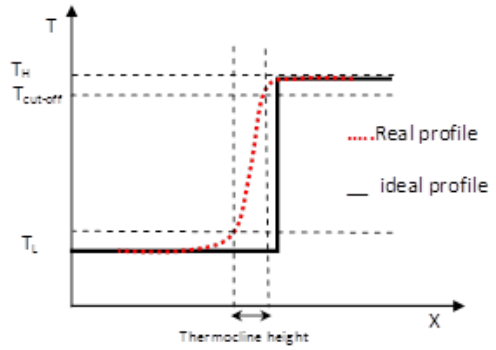

Fig. 2. Real profile, ideal profile and concept of thermocline zone thickness

Fig.2 explains qualitatively the concept of the thermocline zone thickness. The inherently imperfect heat exchange between the solid particles and the fluid leads to a gradual drop in the outlet temperature of the fluid. In practice, this effect prevents the obtaining of the ideal profile since this temperature depends on the conditions of heat exchange with the solid particles of the upper part initially at TH.

As result, the fluid outlet temperature begins to decrease as a function of time to a $T_{cut-off}$ temperature. For a good efficiency, it is desirable to succeed in restoring the maximum amount of heat transfer fluid at high temperature TH. If discharging process occurs with an ideal thermocline temperature profile, the energy returned is maximal. Then, higher the thickness of thermocline zone is, lower the energy discharged is. In our case, to compare the two TESMs, the commons points for both TESM is the discharge time during which the fluid outlet temperature is higher than the Tcut-off temperature for the same height of the storage tank. Therefore, the HTF speed through the packed bed for each TESM must be calculated separately to have the same discharge period.

The HTF axial temperature distribution during charge and discharge for Hitec XL combination with both TESM are plotted in fig. 3. Whereas, fig. 4. presents the HTF temperature distribution, during the discharge process for Delco Term oil combinations. This confrontation is made considering the same size of the storage tank (diameter and height) and the same discharging period (5 hours) where the outlet fluid temperature remains higher than the Tcut-off temperature required by the process.

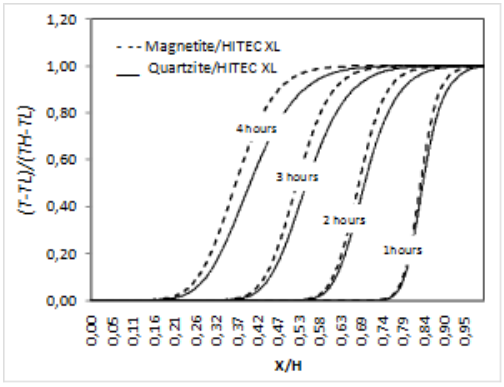

Fig. 3. Numerical HTF temperature profile during charging process for Quartzite/Hitec XL (U=0.000385 m/s) and Magnetite/ Hitec XL (U=0.000572m/s): (a): charge period (b): discharge period. For both TESM, the discharge period is fixed to 5 hours and the storage tank height at 4 m

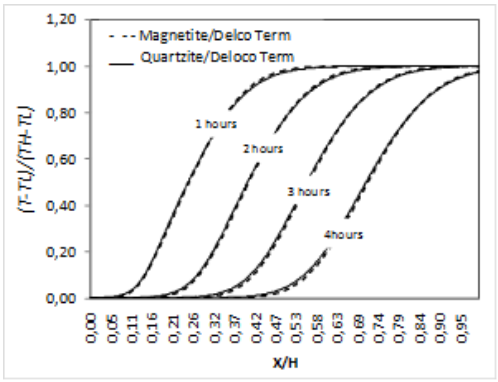

Fig. 4. Numerical HTF temperature profile during charging and discharging process for Quartzite/Delco Term (U=0.000486 m/s) and Magnetite/Delco Term (U=0.000771 m/s):discharge period. For both TESM, the discharge period is fixed to 5 hours and the storage tank height at 4 m.

In that sense and according to fig. 3 and 4, it should be noted that all the HTF temperature profiles resulting from magnetite or quartzite combinations are composed of three essentials regions; the hot region, the thermocline region and the cold one. Also, it appears that when a tank height is fixed as well as the discharge period (5 hours), during which the outlet temperature of the fluid is higher than the $T_{cut-off}$ temperature, Magnetite has a thermocline thickness slightly lower and then closer to the ideal profile for molten salts type HTF combinations (Fig. 3.). Also, we note that the magnetite requires a HTF speed higher than that required by the quartzite to ensure the same period of discharge. Consequently, the energy restored in the case of magnetite will be higher for the same size of the storage tank (height and diameter), since the fluid flow is higher. These results are confirmed even when considering the same HTF speed for both TESMs (Fig. 5). It should be noted that the temperature profile of the magnetite has 1 hour of delay. In other words, for the same HTF speed, the use of quartzite allows faster charging and discharging of the same amount of energy.

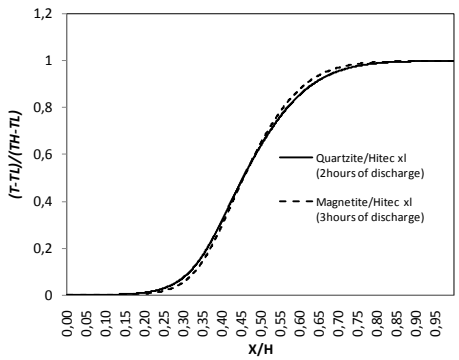

Fig. 5. Numerical HTF temperature profile during discharging process for Quartzite and Magnetite. Delco Term as HTF. For both TESM, the fluid speed is fixed to v=0.00045 m/s and the storage tank height is 4m.

B. TES performances

Numerical performances results for a fixed storage volume (first scenario) are respectively plotted in Table V and VI. From these results, it appears that for a fixed storage tank and discharge period, the quartzite has better thermocline storage performances in terms of discharge efficiency. On the other hand, the energy discharged during the same period by the magnetite exceeds largely the discharged energy by the quartzite. This is not a paradox since the calculated discharge efficiencies take into account the ratio between the energy absorbed by the HTF and the ideal energy referenced to the same TESM. To clarify, for the same storage volume, the magnetite absorbs more energy during the charging process as well as it delivers more energy during the discharge process. However, the corresponding mass flow rate of the HTF required for ensuring the same discharge period is higher. The cycle efficiency cannot offer significant differences since it reflect only the heat losses toward the external medium during charge/discharge cycle. Also, it appears that the nature of the HTF used plays the same role as the TESM: the coupling with a molten salt HTF, which has essentially the larger heat capacity, offers for both TESM better performances compared to the ordinary thermal oil.

For the second scenario, the comparison results in terms of discharged energy, discharge efficiency, and cycle efficiency are presented in Table IV , Table V and Fig. 6 and Fig. 7. It can be observed that significant results have been obtained. Thereby, we can argue that the first important finding concerns the cycle efficiency. For all combinations, the quartzite efficiency seems to be closed to the magnetite efficiency; the difference does not exceed 2%. As mentioned above, the cycle efficiency cannot offer significant differences between combinations since it reflect principally the heat losses toward external medium during one cycle of charge/discharge. For discharge efficiency, the quartzite has the advantage. But in all cases the differences do not exceed 3% between magnetite and quartzite combinations. These results permit to recognize that quartzite combinations present slightly better performances than magnetite combinations. Obviously, combining quartzite or magnetite with molten salt Hitec XL or Hitec HTS can be considered as the most beneficial one.

On the other hand, for the same scenario, regarding the discharged energy reported to the storage volume (fig. 5), the comparison results are inversed since the storage volume required by the quartzite as TESM is significantly higher.

TABLE IV. NUMERICAL PERFORMANCES RESULTS FOR A FIXED STORAGE VOLUME OF 24,54 M3(H=5M) AND DISCHARGE PERIOD OF 5 HOURS

Combinations	Velocity (m/s)	Mass flow (kg/min)	Discharged energy (kWh)	$\eta_{discharg}$	η_{cycle}
(a) Quartzite + Colza oil	5,8E-04	2,278	397	82%	85%
(c) Quartzite + Delco Term E15	6,16E-04	2,269	387	82%	86%
(d) Magnetite + Delco Term E15	9,83E-04	3,62	623	80%	86%
(i) Quartzite+ Hitec HTS	5,.3E-04	4,797	506	88%	85%
(j) Magnetite + Hitec HTS	7,73E-04	7,365	776	88%	85%

TABLE V. CHARACTERISTIC OF THE THERMOCLINE STORAGE TANK FOR THE SECOND SCENARIO: THE STORAGE VOLUME IS CALCULATED FOR EACH COMBINATION BASED ON THE ENERGY REQUIRED (100 KW). THE DISCHARGE PERIOD IS FIXED TO 5 HOURS

Combinations	Storage tank volume (m^3)	Storage tank height (m)	Velocity (m/s)	Mass flow (kg/min)
(b) Magnetite + Colza oil	15,51	4,29	7,860E-04	7,860E-04
(d) Magnetite + Delco Term E15	15,748	4,312	8,370E-04	8,370E-04
(h) Magnetite + Hitec XL	13,644	4,111	5,890E-04	5,890E-04
(i) Quartzite+ Hitec HTS	21,34	4,772	4,810E-04	4,810E-04
(j) Magnetite + Hitec HTS	13,916	4,138	6,330E-04	6,330E-04

Then, unlike the previous results, conducted simulation leads to notable difference between the two filler material from this point of view, combinations based on magnetite as TESM present higher discharged energy per volume unit than quartzite one. Based on these results, it should be pointed out that the cost effective generated by each TESM represents a clear cut for the choice between magnetite and quartzite. In that sense, it seems that this last criterion is probably advantageous for the magnetite.

The second important finding from the aforementioned results is that the nature of the HTF plays the same role as the

TESM: the coupling with a molten salt HTF, which has essentially the larger thermal capacity, expressed by the product of the density and the specific heat, offers for both TESM better performances compared to the ordinary thermal oil. On the other hand, it is known by community working in this field that the TESM thermal capacity is considered one of the most important criteria to bear in mind while choosing a TESM for a thermocline system.

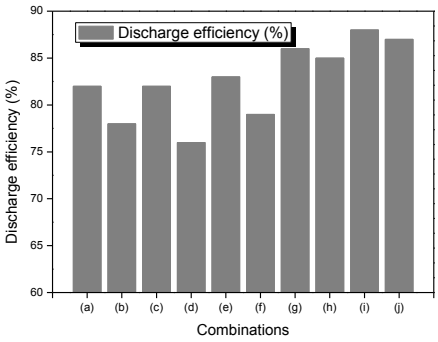

Fig. 6. Discharge efficiency results for the second scenario: the storage volume is calculated for each combination based on the energy required (100 KW). The discharge period is fixed to 5 hours.

Nevertheless, the results mentioned above show that this propriety acts in a paradoxical way regarding the discharge efficiency, since the quartzite represents better performances while magnetite owns largely higher thermal capacity. From thermal point of view, this is explained by the fact that the thermal capacity of the quartzite is the closest to the thermal capacity of both heat transfer fluid tested her. In other word, the gap reduction in thermal capacity between the TESM and the HTF facilitate the energy exchange during charging and discharging process.

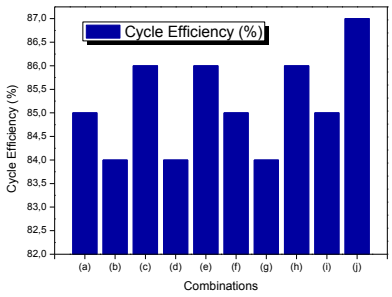

Fig. 7. Cycle efficiency results for the second scenario: the storage volume is calculated for each combination based on the energy required (100 KW). The discharge period is fixed to 5 hours.

ACKNOWLEDGMENT

The authors acknowledge the financial support of IRESEN (Morocco) and KIC InnoEnergy in the framework of SIROCCO-MAGHRENOV project. The authors express their sincere thanks the CIC energigune research center, particularly the Thermal Energy Storage group.

REFERENCES

[1] Meseret Tesfay and Meyyappan Venkatesan,Simulation of thermocline thermal energy storage system using C, International Journal of Innovation and Applied Studies ISSN 2028-9324 Vol. 3 No. 2 June 2013, pp. 354-364.

[2] Albert Graells Vilella,“Analysis of heat storage with a thermocline tank for concentrated solar plants,Proposal of a simulation model and design of an alternative storage system for AndaSol I solar plant”, Sabanci University Industrial Engineering Spring semester 2014.

[3] Antoni, G., et.al, “State of art on high temperature thermal energy storage for power generation part 1-Concepts, materials and modellization”, Renewable and Sustainable Energy Reviews, 14 (2010) 31–55, 2010.

[4] Karthik Nithyanandam, “Investigations on Latent Thermal Storage Systems for Concentrating Solar Power”, Dissertation , the Faculty of the Virginia Polytechnic Institute and State University, May 13, 2013 , Blacksburg, Virginia.

[5] Guruprasad Alva, Lingkun Liu, Xiang Huang, Guiyin Fang, Thermal energy storage materials and systems for solar energy applications, Renewable and Sustainable Energy Reviews 2017; 68: 693-706.

[6] Modi, A., & Perez-Segarra, C. D. (2014). Thermocline thermal storage systems for concentrated solar power plants: One-dimensional numerical model and comparative analysis. Solar Energy, 100, 84-93. DOI:10.1016/j.solener.2013.11.033

[7] J.E. Pacheco, S.K. Showalter, W.j. kolb, Development of a molten-Salt thermocline thermal storage system for parabolic trough plants, J; Solar Energy Eng. 124 (2002) 153-159

[8] J.-F. Hoffmann, T. Fasquelle, V. Goetz, X. Py. A thermocline thermal energy storage system with filler materials for concentrated solar power plants: Experimental data and numerical model sensitivity to different experimental tank scales. Applied Thermal Engineering 100 (2016) 753–761.

[9] J.-F. Hoffmann, T. Fasquelle, V. Goetz, X. Py, Experimental and Numerical Investigation of a Thermocline Thermal Energy Storage Tank, Applied Thermal Engineering (2016), doi: http://dx.doi.org/10.1016/j.applthermaleng.2016.12.053.

[10] Rachid Tiskatine, Ahmed Aharoune, Lahcen Bouirden, Ahmed Ihlal. Identification of suitable storage materials for solar thermal power plant using selection methodology. Applied Thermal Engineering 117 (2017) 591-608.

[11] H. Singh, R.P. saini, A review on packed bed solar energy storage systems, Renew. Sustain. Energy. 14 (3) (2010) 1059-1069.

[12] The engineering ToolBox, Tools and Basic Information for Engineering and Design of Technical Applications. http://www.engineeringtoolbox.com (accessed 2016).

[13] V.A. Salomoni, C.E. Majorana, G.M. Giannuzzi, A.Miliozzi, R. Di Maggio, F. Girardi, D. mele, M. Lucentini, Thermal storage for sensible heat using concrete modules in solar power plants, Sol. Energy 103 (2014) 303-315.

[14] D. McDonnell, 10MWe solar thermal contral receiver pilot plant, mode 5 (test 1150) and mode 6 (test 1160), test report, SAND86-8175-1986.

[15] Brad M. Brown, Matt N. Strasser, R. Paneer Selvam. Development of a structured thermocline thermal energy storage system, Department of Civil Engineering 4190 Bell Engineering Center Fayetteville, Arkansas, USA.

[16] S.E. Faas, L.R. Thorne, E.A. Fuchs, N.D. Gilbertsen. 10MWe solar thermal contral receiver pilot plant: thermal storage subsystem evaluation – final report, SAND86-8212-1986.

[17] S. Khare, M. Dell Amico, C. Knight, S. McGarry, Selection of materials for materials for high temperature sensible energy storage, Sol.Energy Mater. Sol. Celles 115 (2013) 114-122.

[18] S.Kuravi, J. Trahan, D.Y. Goswami, M.M. Rahman, E.K. Stefanakos, Thermal energy storage technologies and systems for concentrating solar power plants, Prog, Energy Comust. Sci 39 (2013) 285-319

[19] M.E. Navarro, M. Martinez, A. Gil, A.I. Fernandez, L.F. Cabeza, R.Olives, X. Py, Selection and characterization of recycled materials for sensible thermal energy storage, Sol. Energy Mater. Sol. Cells 107 (2012) 11-135.

[20] X. Py, N. Calvet, R. Olivès, P. Echegut, C.Bessada, F. Jay, Thermal storage for solar power plants based on low cost recycled material, Proceeding pf the 11th International Conference on TES, Stockholm, Sweden, 2009.

[21] D. Laing, S. Zunft, Using concrete and other solid storage media in thermal energy stirage (TES) systems, Adv. Therm. Energy Storage Syst. (2015) 65-86.

[22] N. Calvet, J. Gomez, A. Starace, A. Meffre, G. Glatzmaier, S. Doppiu, X. Py, Compatibility of low-cost recycled ceramics with nitrate molten salts for a sustainable active direct thermocline storage system, Proceeding of the 12th International Conference on energy Storage, 2012.

[23] D. Laing, D. Lehmann, M. Fiss, Test results of concrete thermal energy storage for parabolic trough power plants, J. Sol. Energy Eng. 131 (4) (2009) 041007.

[24] W. Loop, D. Water, Standard Test Method for Water Absorption, Bulk Density, Apparent Porosity, and Apparent Specific Gravity of Fired Whiteware Products 1,88, 2006, pp. 1–2.

[25] Chao Xu et al. Sensitivity analysis of the numerical study on the thermal performance of a packed-bed molten salt thermocline thermal storage system. Int. J. of Applied Energy.

[26] J.F Hoffman, "Stockage thermique pour centrale solaire thermodynamique à concentration mettant en œuvre des matériaux naturels ou recyclés ", thèse de doctorat, Université de Perpignan (2015).

[27] Erick Guadamud, Ahmed Al Mers, Jorge Chiva, Guillem Colomer, Joan Farnós, Joaquim Rigola and Carlos David Perez-Segarra, *Development of a high accurate numerical platform for the thermal and optical optimization of linear Fresnel receivers*, ISES SOLAR WORLD CONFERENCE 2017 (29 Oct - 2 Nov Abu Dhabi, UAE).